


RESEARCH ARTICLE

WILEY

Receptor–ligand and parasite protein–protein interactions in *Plasmodium vivax*: Analysing rhoptry neck proteins 2 and 4

Maritza Bermúdez^{1*} | Gabriela Arévalo-Pinzón^{1,2*} | Laura Rubio¹ | Olivier Chaloin³ | Sylviane Muller^{3,4,5} | Hernando Curtidor^{1,6} | Manuel Alfonso Patarroyo^{1,6} 

¹ Fundación Instituto de Inmunología de Colombia (FIDIC), Bogotá, Colombia

² PhD Programme in Biomedical and Biological Sciences, Universidad del Rosario, Bogotá, Colombia

³ CNRS, Immunopathology and therapeutic chemistry, Institut de Biologie Moléculaire et Cellulaire (IBMC), Strasbourg, France

⁴ CNRS, Biotechnology and cell signaling, University of Strasbourg, France / Laboratory of Excellence Medalis, France

⁵ University of Strasbourg Institute for Advanced Study (USIAS), Strasbourg, France

⁶ School of Medicine and Health Sciences, Universidad del Rosario, Bogotá, Colombia

Correspondence

Manuel Alfonso Patarroyo, Fundación Instituto de Inmunología de Colombia (FIDIC), Carrera 50 # 26-20, Bogotá, Colombia. Email: mapatarr.fidic@gmail.com

Funding information

Departamento Administrativo de Ciencia, Tecnología e Innovación (Colciencias), Grant/Award Number: RC#0309-2013; Initiative of Excellence (IdEx); Laboratory of Excellence Medalis, Grant/Award Number: ANR-10-LABX-0034; French Centre National de la Recherche Scientifique (CNRS)

Abstract

Elucidating receptor–ligand and protein–protein interactions represents an attractive alternative for designing effective *Plasmodium vivax* control methods. This article describes the ability of *P. vivax* rhoptry neck proteins 2 and 4 (RON2 and RON4) to bind to human reticulocytes. Biochemical and cellular studies have shown that two PvRON2- and PvRON4-derived conserved regions specifically interact with protein receptors on reticulocytes marked by the CD71 surface transferrin receptor. Mapping each protein fragment's binding region led to defining the specific participation of two 20 amino acid-long regions selectively competing for PvRON2 and PvRON4 binding to reticulocytes. Binary interactions between PvRON2 (ligand) and other parasite proteins, such as PvRON4, PvRON5, and apical membrane antigen 1 (AMA1), were evaluated and characterised by surface plasmon resonance. The results revealed that both PvRON2 cysteine-rich regions strongly interact with PvAMA1 Domains II and III (equilibrium constants in the nanomolar range) and at a lower extent with the complete PvAMA1 ectodomain and Domains I and II. These results strongly support that these proteins participate in *P. vivax*'s complex invasion process, thus providing new pertinent targets for blocking *P. vivax* merozoites' specific entry to their target cells.

KEYWORDS

malaria, *Plasmodium vivax*, reticulocytes, rhoptry neck proteins, synthetic peptide

1 | INTRODUCTION

The invasion cycle of parasites from the phylum Apicomplexa (i.e., *Toxoplasma gondii* or *Plasmodium* spp) represents one of the most complex pathogen invasion processes that is actively orchestrated by the parasite itself through a series of events involving a diverse set of molecular interactions (Carruthers, 2002; Weiss, Crabb, & Gilson, 2016). Such process requires a sequence of coordinated activities, including recognition, host cell attachment, protein secretion (from micronemes and rhoptries) and motility, supported by an actin-/myosin-based gliding in Apicomplexan parasites (Weiss et al., 2015). One of its most outstanding features concerns the formation of stable, high-avidity merozoite (Mz) apex binding to a host cell,

resembling a form of ring moving progressively (moving junction [MJ]) from the apical pole towards the back of the parasite, propelling it into a nascent parasitophorous vacuole, thereby allowing it to survive and replicate within a target cell (Aikawa, Miller, Johnson, & Rabbege, 1978).

Studies orientated towards identifying the components forming the circumferential ring have shown that it appears to be mainly formed by a multimeric protein complex, involving the parasite's apical membrane antigen 1 (AMA1) and rhoptry neck (RON) proteins -2, -4, -5, and -8 (the latter only in *T. gondii*) (Alexander, Mital, Ward, Bradley, & Boothroyd, 2005; Besteiro, Michelin, Poncet, Dubremetz, & Lebrun, 2009; Collins, Withers-Martinez, Hackett, & Blackman, 2009; Straub, Cheng, Sohn, & Bradley, 2009). The RON/AMA1 complex acts independently of host cell receptors as Apicomplexans secrete RON proteins into a host cell, using RON2 as receptor on target cell

*These authors are equal contributors.

membrane. RON2 is anchored to host cell surface, and the carboxyl terminal region remains exposed for binding to AMA1, which acts as parasite ligand (Besteiro et al., 2009; Lamarque et al., ; Srinivasan et al., 2011). Regarding the other RONs, it has been described that RON5 and RON8 in *T. gondii* are involved in stabilising and organising the complex in a host cell (Beck, Chen, Kim, & Bradley, 2014; Straub, Peng, Hajagos, Tyler, & Bradley, 2011). It has been found that conditional knockdown involving a loss of TgRON5 has led to the complete degradation of TgRON2 and mistargeting of TgRON4 (Beck et al., 2014), whereas a loss of TgRON4 has significantly reduced TgRON5 and TgRON2 levels (Guerin et al., 2017). It has also been shown that four host proteins (ALIX-CD2AP-CIN85 and TSG101) are specifically recruited to the MJ through specific binding motifs present on TgRON proteins (Guerin et al., 2017).

Structural studies of the complex formed between AMA1 and a RON2 peptide have shown the participation of the AMA1 hydrophobic trough, so that a binding pocket accepts the RON2 critical loop region, having significant shape and complementary charge (Tonkin et al., 2011; Vulliez-Le Normand et al., 2012; Vulliez-Le Normand, Saul, Hoos, Faber, & Bentley, 2017). This interaction's importance in *Plasmodium falciparum* has been established by using antibodies, peptides, or small molecules directed against the PfAMA1-PfRON2 complex interface, thereby significantly inhibiting invasion (Collins et al., 2009; Lamarque et al., ; Srinivasan et al., 2013). Immunising mice with the AMA1-RON2L complex (but not with individual antigens) has induced qualitatively higher growth inhibitory antibodies capable of protecting mice against experimental challenge with a lethal *Plasmodium yoelii* strain, highlighting such protein–protein interaction's important role during invasion (Srinivasan et al., 2014).

AMA1 was initially identified in *Plasmodium knowlesi* (Deans et al., 1982) and then found throughout all Apicomplexa, being essential for *T. gondii* and *P. falciparum* survival (Mital, Meissner, Soldati, & Ward, 2005; Triglia et al., 2000). Regarding AMA1's function in MJ formation, various roles involved in *P. falciparum* invasion have been attributed to it, including Mz reorientation on red blood cell (RBC) surface (Mitchell, Thomas, Margos, Dluzewski, & Bannister, 2004), participation in resealing RBC at the end of invasion (Yap et al., 2014), interaction with aldolase that provides extracellular linkage for the actin/myosin motor (Diaz et al., 2016), and interaction with receptors on RBC surface (Kato, Mayer, Singh, Reid, & Miller, 2005; Urquiza et al., 2000). Previous observations showed that tachyzoites (Tz) and sporozoites (Spz) having conditional knockouts for AMA1 were capable of invading a host cell and appeared to form normal MJ, suggesting that AMA1 was acting independently of RONs and that AMA1–RON2 interaction was not essential (Bargieri et al., 2013; Giovannini et al., 2011). However, later studies showed that Tz used paralogues of the generic AMA1–RON2 pair as substitutes, partially compensating for the loss of TgAMA1 (Lamarque et al., 2014). Alternative pathways for the lack of AMA1 and RON2 have not been reported in *P. falciparum* (Lamarque et al., 2014), unlike that observed in other invasion steps (such as reorientation) using functionally redundant proteins, such as erythrocyte binding antigens (EBAs) and reticulocyte-binding-like protein homologues (RH; Lopatnicki et al., 2011). This would suggest that although it might be a conserved mechanism amongst Apicomplexa, differences

concerning regulation of MJ components, composition, and interaction regions could partly define selectivity by their respective host cells.

P. falciparum RONs were identified by coimmunoprecipitation assays showing AMA1 association with high molecular weight components located in the rhoptry neck (Curtidor, Patino, Arevalo-Pinzon, Patarroyo, & Patarroyo, 2011) homologues of those reported in *T. gondii* (Alexander, Arastu-Kapur, Dubremetz, & Boothroyd, 2006; Bradley et al., 2005; Cao et al., 2009). Even though there is no clear evidence of PfRON2, PfRON4, and PfRON5 translocation across/onto host cell membrane and RBC cytosol in *P. falciparum*, previous studies have shown that PfRON2 uses a cysteine-rich region (PfRON2-C) located in the carboxyl terminal extreme for interacting with receptors on a host cell; these are sensitive to treatment with trypsin and neuraminidase (Hossain, Dhawan, & Mohammed, 2012). However, the cysteine-rich region located in PfRON2's central portion (PfRON2-M) and the PfRON2-C region interact with PfAMA1 (Hossain et al., 2012). PfRON5 contains peptides having high affinity binding to receptors on RBC, which are capable of inhibiting Mz entry to target cells. Such data highlight RON and AMA1 participation in establishing receptor–ligand and protein–protein interactions (Counihan, Kalanon, Coppel, & de Koning-Ward, 2013; Remarque, Faber, Kocken, & Thomas, 2008).

Regarding *Plasmodium vivax*, the geographically most widespread cause of human malaria (Howes et al., 2016), there is little information concerning the proteins participating in binding (ligand–receptor interaction) or protein–protein interactions, partly due to difficulties in culturing *P. vivax* in vitro thereby impeding genetic approaches for studying proteins' role during the cycle of invasion of reticulocytes. Such limitations have been a barrier to studying the biological, clinical, and immunological characteristics necessary for designing control measures against *P. vivax*. Using *P. vivax* strains adapted in non-human primates (Pico de Coana et al., 2003) or infected patients' blood (Bozdech et al., 2008) has enabled comparative approaches with other *Plasmodium* species (Patarroyo, Calderon, & Moreno-Perez, 2012) or using omic sciences (Moreno-Perez, Degano, Ibarrola, Muro, & Patarroyo, 2014; Venkatesh et al., 2016) to identify a significant amount of proteins expressed in *P. vivax* schizonts (Sch) and Mz (Patarroyo et al., 2012). PvRON2 (Arevalo-Pinzon, Curtidor, Patino, & Patarroyo, 2011), PvRON4 (Arevalo-Pinzon, Curtidor, Abril, & Patarroyo, 2013), and PvRON5 (Arevalo-Pinzon, Bermudez, Curtidor, & Patarroyo, 2015) have been identified recently; these are homologous to those identified in *P. falciparum*, which are located in the apical extreme of *P. vivax* Colombia Guaviare 1 (VCG-1) strain Sch. Different biochemical techniques have been used to report a conserved PvRON5 fragment located towards the carboxyl-terminal extreme interacting with RBC, having a preference for CD71⁺ cells (Arevalo-Pinzon et al., 2015), suggesting that RONs could be participating in host–parasite interactions, similar to that found in *P. falciparum*.

PvRON2 and PvRON4 ability to interact specifically with RBC was thus evaluated to advance the functional characterisation of *P. vivax* RONs; this was followed by determining binary interactions between PvRON2, PvRON4, PvRON5, and PvAMA1 by surface plasmon resonance (SPR). The data indicate that the PvRON2 central and PvRON4 carboxyl terminal regions specifically interact with protein receptors

on reticulocyte membrane having CD71⁺CD45⁻ phenotype. It was also shown here that PvRON2 also participates in interaction with other parasite proteins, such as PvAMA1, PvRON4, and PvRON5, highlighting *P. vivax* RON participation in establishing several protein–protein and host–pathogen interactions.

2 | RESULTS AND DISCUSSION

2.1 | The PvRON4 carboxyl terminal region interacted with umbilical cord blood RBC

Recombinant plasmids were constructed based on evidence regarding two *P. falciparum* RON2 cysteine-rich regions' binding and interaction activity (Hossain et al., 2012; Lamarque et al.,); they contained the regions encoding the *P. vivax* central (PvRON2-RI) and carboxyl terminal (PvRON2-RII) regions (Figure 1a). A PvRON4 region located towards the carboxyl terminal extreme was amplified (Figure 1a); it is highly conserved at intraspecies and interspecies level and is under purifying selection, contrary to that reported for the amino terminal region having extensive size polymorphism (Buitrago, Garzon-Ospina, & Patarroyo, 2016). Selected regions were cloned in pRE4 vector in frame with herpes simplex virus (HSV) glycoprotein D signal peptide and transmembrane domain thereby enabling proteins to be expressed and anchored to cell membrane (Cohen et al., 1988). Following transfection and

immunofluorescent studies on nonpermeabilised cells, it was found that only PvRON4 was correctly and efficiently expressed on COS-7 cell membrane (Figure 1b). Several modifications to COS-7 cell transfection and expression protocols for PvRON2-RI and PvRON2-RII fragments led to low transfection and expression efficiency compared with that obtained with PvRON4 and PvDBP-RII recombinant fragments. It should be noted that some transient transfections in COS-7 cells may have relatively low protein expression rates, as has been reported previously for other proteins (Berntzen et al., 2005).

The *P. vivax* infection has been seen to be limited to Duffy (Fy) positive reticulocytes, also known as the Duffy antigen/receptor for chemokines (DARC). Such preference seems to be mediated by specific receptor–ligand interactions between the DBP protein expressed by the parasite and the DARC receptor on RBC membrane (Miller, Mason, Clyde, & McGinniss, 1976). DBP–DARC interaction was taken as positive control based on the above information where PvDBP cysteine-rich Region II was expressed on COS-7 cell membrane (Figure 1b). As expected, PvDBPRII interacted with DARC whilst having low negative Duffy cell binding capacity, ANOVA-Tukey: $F(3, 12) = 24.8$, $p < .0001$ (Figure 1b,c). The PvRON4 C-terminal cysteine-rich region (pRE4-PvRON4 construct) bound to umbilical cord blood (UCB) RBC having different Duffy phenotypes, although their binding activity was lower than that found for PvDBP-RII (Figure 1b,c). PvRON4 binding to Fy⁺Fy⁻ had statistically significant differences regarding binding to Fy⁻Fy⁻ RBC, ANOVA-Tukey: $F(3, 12) = 4.26$, $p = .020$. When

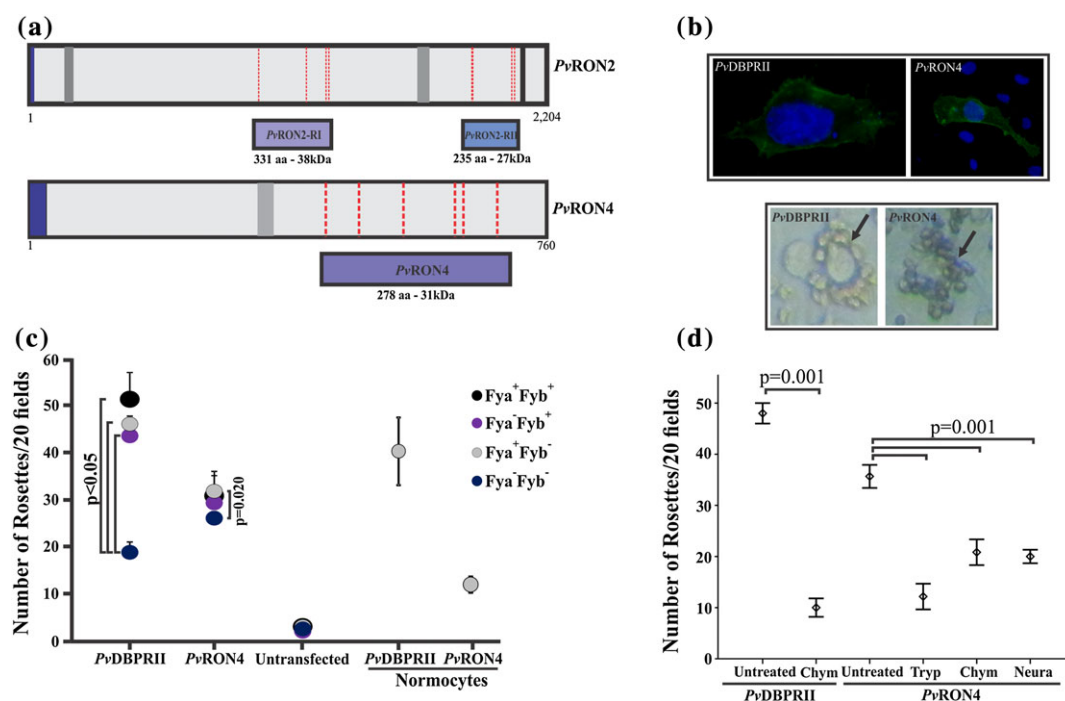


FIGURE 1 PvRON4 binding to RBCs. (a) PvRON2 and PvRON4 schematic representation. Each protein's main characteristics are shown. Signal sequence (dark blue), transmembrane domains (black), coiled-coil domains (grey), and cysteine residues conserved amongst *Plasmodium vivax* strains (dotted red lines) (Arevalo-Pinzon et al., 2011; Arevalo-Pinzon, Curtidor, Abril, & Patarroyo, 2013). The locations are shown of two PvRON2 fragments (PvRON2-RI and PvRON2-RII) and one PvRON4 fragment, which were cloned in vectors to be expressed in COS-7 cells and *Escherichia coli*. (b) PvDBPRII and PvRON4 expression and location on COS-7 eukaryote cell surface. Above: Green shows expressed proteins and blue shows DAPI-stained cell nuclei. Transfection efficiency was ~5%, which was used for normalising the Rosetting data. Below: An example of a rosette indicating RBC bound to COS-7 cell surface. (c) Rosette formation assay. Computation of the amount of rosettes counted in 20 fields using UCB RBC from different Duffy phenotypes with COS-7 cells transfected with PvDBPRII or PvRON4. A rosette assay involving normocytes having Fy⁺Fy⁻ phenotype was also included (d) Enzyme treatment assays. The amount of rosettes formed between cells transfected with PvDBPRII or PvRON4 and UCB RBC treated with different enzymes is shown. All Rosetting assays were performed three times in triplicate

PvRON4 binding to RBC ($m = 34 \pm 2.7$) was compared with binding to normocytes ($m = 11 \pm 1.4$), it was observed that the amount of rosettes compared with normocytes became significantly reduced, t test: $t(10) = 18.68$, $p = .001$ (Figure 1b,c). This suggested that PvRON4 binding to RBC depends on a more immature RBC population, similar to that reported for other *P. vivax* antigens, such as PvAMA1 (Arevalo-Pinzon, Bermudez, Hernandez, Curtidor, & Patarroyo, 2017), PvGAMA (Baquero et al., 2017), and EBP2 (Ntumngia et al., 2016), whereas PvDBPRII bound to both RBC and normocytes (Figure 1c).

Several reports have shown that different *P. falciparum* strains differ regarding their ability to invade RBC treated with different enzymes, such as trypsin, chymotrypsin, and neuraminidase, removing different receptors from RBC surface (Duraisingh et al., 2003; DeSimone et al., 2009). Such assays enabled ascertaining that proteins like erythrocyte binding antigen 175 (EBA175) recognised the sialic acid component in glycophorin A (Duraisingh, Maier, Triglia, & Cowman, 2003) and EBA 140 bound to glycophorin C (Gilberger et al., 2003). It has been reported (and also found here) that PvDBP binding to DARC was susceptible to enzymatic treatment with chymotrypsin (Barnwell, Nichols, & Rubinstein, 1989), t test: $t(4) = 24.4$, $p = .001$ (Figure 1d). It has also been reported that PvAMA1 binding was susceptible to neuraminidase and chymotrypsin action (Arevalo-Pinzon et al., 2017). Interestingly, it was found here that PvRON4 interacted with RBC membrane protein receptors susceptible to treatment with the three enzymes evaluated, ANOVA-Tukey: $F(3, 8) = 59$, $p = .001$ (Figure 1d). Such binding profile did not fit any enzymatic behaviour typical of previously described malaria receptors.

Concerning other parasites such as *T. gondii*, a 17-kDa region in TgRON4 proximal C-terminus was sufficient for binding to host cell β -tubulin carboxyl-terminal region (Takemae et al., 2013). Even though the overall similarity between *T. gondii*, *P. falciparum*, and *P. vivax* RON4 is not very high (Supporting Information), a pattern of conservation could be observed towards these proteins' carboxyl terminal region. This suggested that functional RON4 binding region was located towards this region, even though receptor type differed according to species, as shown by TgRON4 (Takemae et al., 2013) and PvRON4 interaction results (Figure 1). Although it is still not clear whether RON4 is exported towards host cell cytosol, its participation in MJ formation is crucial for target cell invasion by *T. gondii* and *P. falciparum* (Giovannini et al., 2011). Recent studies have found that the PvRON4 central region contained a sterease/lipase domain, which could be associated with ester bonds rupture in the phospholipids constituting host cell membrane (Buitrago et al., 2016). This suggested the presence of several functional domains in RON4, where the C-terminal region could interact with RBC membrane whilst the sterease/lipase (central region) domain could then enable RON4 internalisation. Future studies aimed at elucidating such functional domains' coordinated involvement in invasion should be carried out.

The mechanism by which proteins such as Tg, Pf, and Pv RON4, RON5, and RON8 are translocated to host cell cytoplasm has not yet been elucidated. It cannot be ruled out that proteins must first interact with proteins on host cell membrane for this to occur, as seen in this PvRON4 study (Figure 1). It has been found that one PvRON5 region and some PfRON5 20 residue-long peptides specifically interact with RBC membrane (Arevalo-Pinzon et al., 2015; Curtidor et al., 2014).

2.2 | PvRON4 and PvRON2-RII bound specifically to CD71-labelled reticulocytes

Three protein fragments were obtained in recombinant form in *Escherichia coli* for determining PvRON4–RBC interaction specificity and evaluating PvRON2-RI and PvRON2-RII specific binding capability (Figure 1a); these regions were then purified by affinity chromatography. A single band was found for each fragment by western blot and Coomassie blue staining, coinciding with the expected molecular weights (Figure 2a, left). The three recombinant fragments contained conserved cysteine residues amongst the different *P. vivax* strains (Arevalo-Pinzon et al., 2011; Arevalo-Pinzon, Curtidor, Abril, & Patarroyo, 2013). Although internal disulphide linkage formation in these fragments is still unknown, previous studies with the RON2sp1 show that disulphide bridge formation between Cys2051–Cys2063 (PvRON2sp1) and Cys2037–Cys2049 (PfRON2sp1) in RON2 carboxy terminal region is important for this peptide's interaction with the AMA-1 hydrophobic groove (Vulliez-Le Normand et al., 2012; Vulliez-Le Normand et al., 2017). Ellman test did not reveal sulphhydryl groups in these fragments, that is, no free thiol groups in any of the three recombinant proteins, indicating disulphide bridges. Thionitrobenzoic acid formation was observed when proteins were incubated with a molar excess of DTT, which is formed only in the presence of free sulphhydryl groups.

Every recombinant fragment was radiolabelled, quantified, and incubated in a UCB RBC competition assay with high concentrations of the same nonradiolabelled recombinant protein. The results showed that even though the three fragments did bind (total binding), only PvRON4 and PvRON2-RI bound specifically to RBC, because radiolabelled protein binding became reduced (by ~55%) in the presence of nonradiolabelled protein (non-specific binding; Figure 2a, right). When graphing specific binding, it was observed that PvRON4 and PvRON2-RI specific binding activity was 1%–PvRON4 to 2.6%–PvRON2-RI (curve slope) compared with PvRON2-RI 0.22% specific activity (Figure 2a, right).

As *P. vivax* Mrz have a strong preference for reticulocytes expressing transferrin receptor 1 (CD71; becoming sequentially lost as reticulocytes mature), cytometry was used for determining whether PvRON4 and PvRON2-RI binding was restricted to interaction with this type of immature cell (reticulocyte stages I–III). Figure 2b shows that PvRON2-RI had 6.56% binding to CD71⁺CD45[−] cells ($m = 7.6 \pm 0.94\%$, 95% CI [5.2, 9.9]) and PvRON4 5.60% ($m = 5.15 \pm 0.55\%$, 95% CI [3.7, 6.5]), whereas low CD71[−]CD45[−] cell interaction (~0.1%) was found (data not shown). PvDBPRII recombinant protein had 10.5% binding (positive control; $m = 12.3 \pm 1.47\%$, 95% CI [8.6, 15.95]) whereas PvDBPRIII–IV recombinant protein, expressing Regions III and IV (negative control), had low binding capacity ($m = 1.0 \pm 0.55\%$, [−0.3, 2.4]), thereby coinciding with previous studies showing that these regions do not participate in target cell binding (Chitnis & Miller, 1994; Ocampo et al., 2002). Although these proteins interacted preferentially with CD71-labelled reticulocytes, the PvRON4 protein receptor's enzymatic profile did not match the CD71 protein profile, indicating that this is not the PvRON4 receptor. It has been reported very recently that CD71 acts as receptor for the PvRBP2b ligand and that interaction is trypsin- and chymotrypsin-sensitive (Gruszczyk et al., 2018).

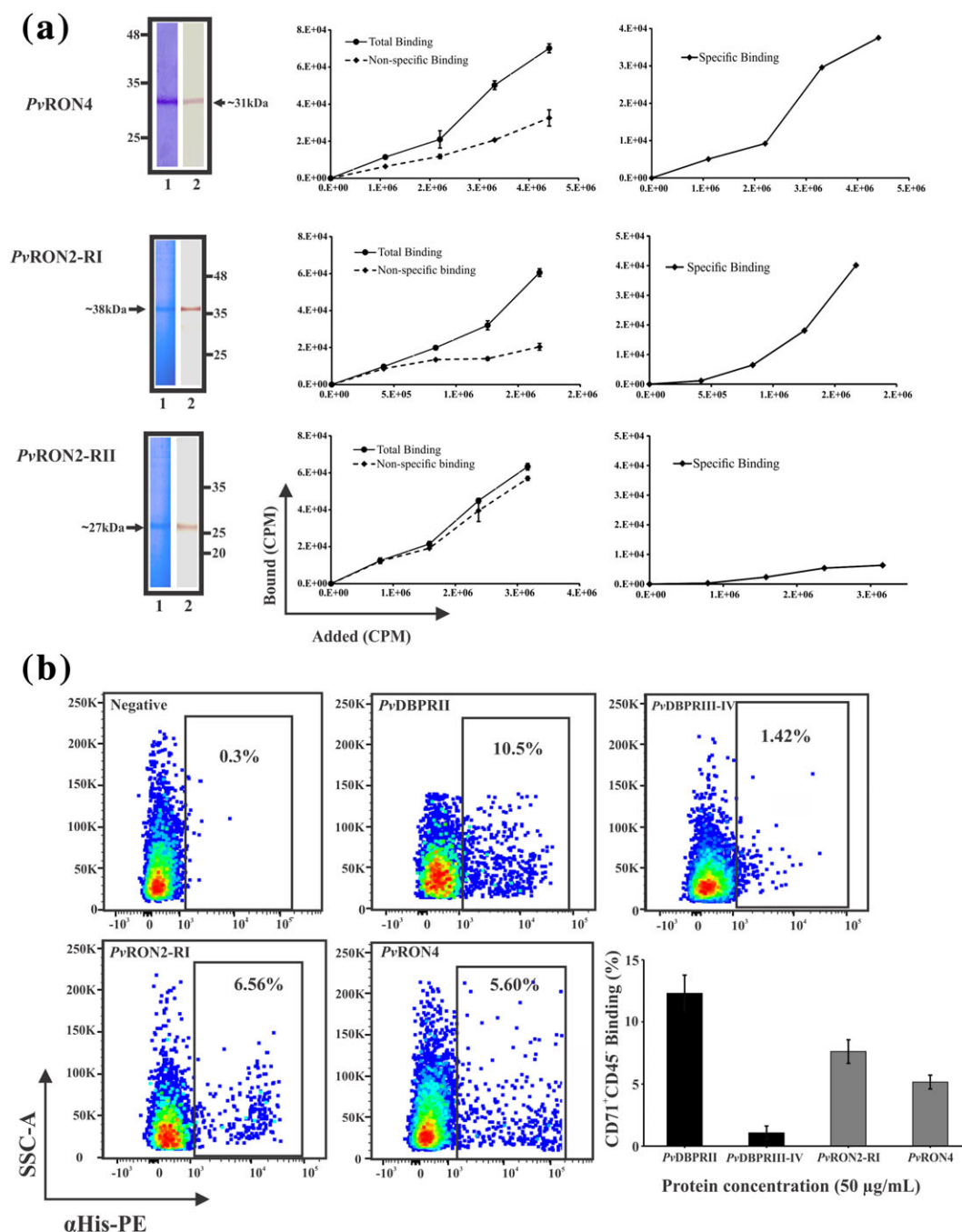


FIGURE 2 PvRON2-RI and PvRON4 proteins interacted specifically with CD71⁺ reticulocytes. (a) PvRON2 and PvRON4 expression and specific binding to UCB RBC. Left-hand side: protein recognition by western blot (1) with monoclonal antihistidine antibody and Coomassie blue staining (2) after the purification of the three proteins obtained in *Escherichia coli*. Right-hand side: specific binding assays. All recombinant proteins were radio-labelled with Na¹²⁵I and made to compete for binding to UCB RBC in the absence (total binding) or presence of the same nonradiolabelled protein (non-specific binding). A specific binding curve was obtained from the two curves. CPM: counts per minute. Data are shown as the mean values (±SD) of at least three independent experiments. (b) PvRON2-RI and PvRON4 binding to CD71⁺CD45⁻ as measured by flow cytometry. Dot plots show the evaluated recombinant proteins' binding to a CD71⁺CD45⁻ reticulocyte population. Binding was detected by a PE-conjugated monoclonal antihistidine antibody. The percentage obtained for negative control (cells without recombinant protein) was subtracted from each binding assay. The bar graph represents each protein's average binding to CD71⁺CD45⁻ cells obtained in three assays performed in triplicate

It has been reported that the PfrON2 fragment involved in interaction with RBC is located in the carboxyl-terminal region (Hossain et al., 2012), different to that found for PvRON2 where, even though both regions bound, only the region located towards the protein's central portion (called PvRON2-RI here) specifically interacted with UCB RBC (Figure 2). Such data, added to that available for *P. vivax* proteins (e.g., PvMSP1 and PvAMA1, Arevalo-Pinzon et al., 2017, and now

PvRON2), have shown that some *P. vivax* proteins having orthologues in *P. falciparum* fulfil the same functions but use different functional regions. This has important implications when designing effective control mechanisms against *P. vivax* malaria and could be partly responsible for the specificity of interaction with respective target cells.

It is still not clear why *P. vivax* has tropism for CD71⁺ reticulocytes; the interaction defined between DBP and DARC was initially

considered essential for parasite binding; however, DARC is expressed on both reticulocytes and erythrocytes. Recent studies have managed to show that DARC epitope recognised by DBP has increased its exposure during early stages of reticulocyte maturation and decreased it during maturation into normocytes (Ovchinnikova et al., 2017). DARC epitope exposure during reticulocyte stages I–III enables greater DBP association with CD71^{high}/TO^{high} reticulocytes, but not in mature reticulocytes or erythrocytes, partly explaining *P. vivax* tropism for reticulocytes (Ovchinnikova et al., 2017). It is worth noting that specific tropism for CD71⁺ reticulocytes has also been shown for other *P. vivax* proteins, including those studied here. Receptor remodelling during reticulocyte maturation, added to the fact that proteins have distinct binding domains in each species, could complement each parasite's selectivity for its respective host cell.

2.3 | Twenty-residue-long peptides were capable of specifically competing for PvRON4 and PvRON2 binding

Competition assays were carried out between peptides covering radiolabelled protein and recombinant protein fragments' amino acid sequences to define the regions responsible for PvRON2 and PvRON4

interaction with CD71⁺CD45[−] cells. The results showed that PvRON4 fragment-derived peptides 40305, 40306, 40312, and 40313 could inhibit recombinant protein binding by 40% (40305; Figure 3a). Three peptides (40592, 40593, and 40595) inhibited PvRON2-RI radiolabelled protein binding by up to 41% (Figure 3b).

Peptides 40305, 40313, 40592, and 40595 were radiolabelled and tested in a RBC binding assay, in the presence or absence of nonradiolabelled peptide for characterising PvRON4 and PvRON2-RI specific binding activity as such peptides were capable of inhibiting recombinant protein binding. This method required peptides having ≥ 0.02 or 2% specific binding activity, according to the specific binding curve, named here high activity binding peptides—HABPs (Rodriguez et al., 2008). This assay gave PvRON4 peptide 40305 and PvRON2-RI 40595 slopes greater than 2% (Figure 3c,d), thereby cataloguing them as HABPs. Flow cytometry showed that HBP 40305 could inhibit protein binding to CD71⁺CD45[−] reticulocytes by up to 23% and HBP 40495 by 40% (Figure 3c,d). HBP 40305 was also able to inhibit rosette formation by 41% compared with negative control (absence of peptide; Figure 3c).

A significant amount of HABPs have been identified in most *P. falciparum* proteins participating in Spz and Mz invasion of their respective target cells (Rodriguez et al., 2008; Curtidor, Vanegas, Alba,

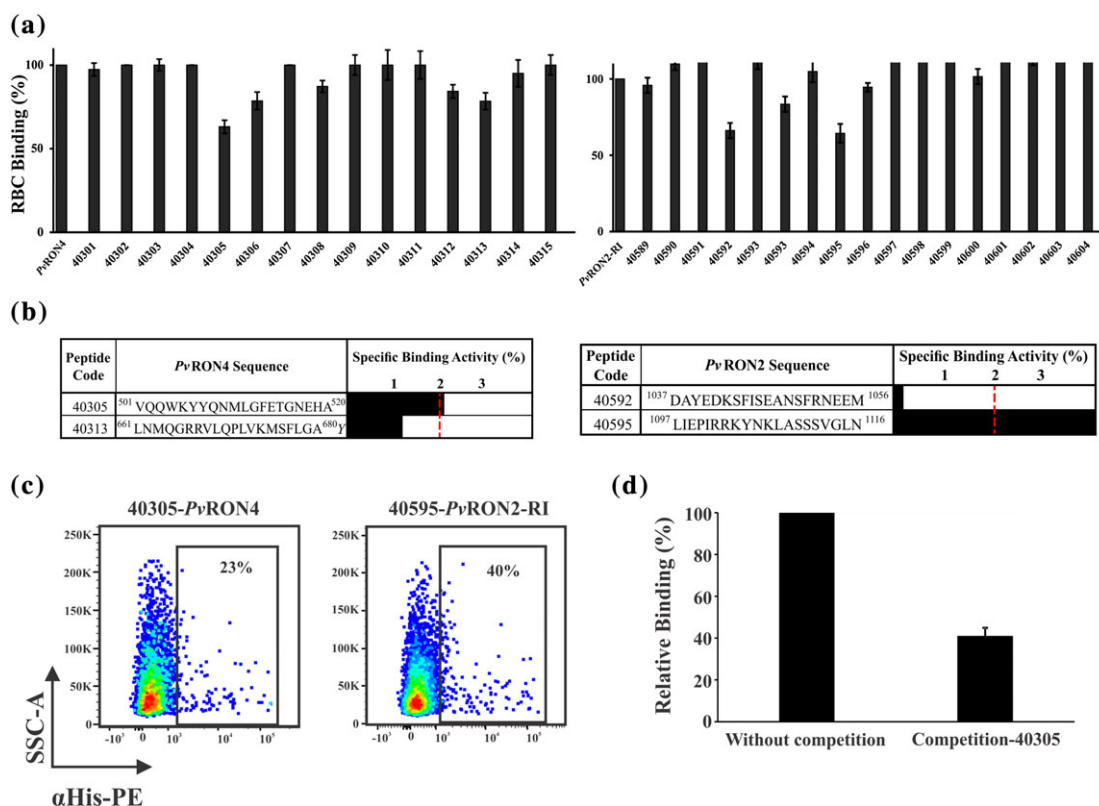


FIGURE 3 Ascertaining PvRON2-RI and PvRON4 RBC binding regions. (a) Competition assays between synthetic peptides and PvRON4 recombinant protein (left) or PvRON2-RI (right) regarding RBC binding. RBC binding percentage in the absence (100% binding) or presence of each synthetic peptide covering each recombinant protein complete sequence (inhibition). Peptides were numbered according to our institute's serial system. Data is shown as mean values (\pm SD) regarding at least 3 independent experiments. (b) Determining PvRON4 and PvRON2 HABPs and competition studies. PvRON4-derived peptides 40305 and 40313 and PvRON2-RI-derived 40592 and 40595 binding profiles. Horizontal black bar length indicates each peptide's specific binding activity. The location of each sequence in PvRON4 or PvRON2 is also shown in superscript. Peptides having specific binding activity equal to or greater than 2% were considered HABPs (Rodriguez et al., 2008). (c) Flow cytometry competition assays. Dot plots of PvRON4 or PvRON2-RI binding to CD71⁺CD45[−] cells in the presence of HABPs 40305 and 40595. Inhibition percentages are indicated regarding protein total binding (100%). (d) Peptide 40305 inhibition of rosette formation on COS-7 cells transfected with PvRON4

& Patarroyo, 2011). After HABPs have undergone a series of chemical modifications and structural and immunological studies, they have been able to induce a strong protection-inducing immune response in experimental challenge in a non-human primate animal model (Curtidor, Patarroyo, & Patarroyo, 2015). Such HABPs have now been defined as immune protection-inducing protein structures (IMPIPS), and some of them are strong candidates for a multiantigen, multistage, subunit-based anti-*P. falciparum* vaccine (Patarroyo et al., 2015). The ~40 proteins identified in *P. vivax* could play important roles during reticulocyte invasion (Patarroyo et al., 2012); PvDBP (Ocampo et al., 2002), PvMSP1 (Rodriguez et al., 2002), PvRBP1 (Urquiza et al., 2002), and PvAMA1 (Arevalo-Pinzon et al., 2017) HABPs had only been identified to date, but now PvRON2 and PvRON4 can be added to the list.

2.4 | Both PvRON2 regions had a high-affinity interaction with PvAMA1 Domains II and III

Previous *P. falciparum* and *T. gondii* immunoprecipitation and confocal microscopy studies have defined an AMA1-RON2-RON4-RON5 macromolecular complex participating in MJ formation (plus RON8 in *T. gondii*). Studies about this complex's stability in denaturing conditions (including sodium dodecyl sulphate) have shown that only the interaction between AMA1 and RON2 is maintained (Besteiro et al., 2009). It has been reported that a 39-residue-long peptide derived from PfRON2, TgRON2, and PvRON2 externally exposed regions specifically interacts with the AMA1 hydrophobic groove (Tonkin et al., 2011; Vulliez-Le Normand et al., 2012; Vulliez-Le Normand et al., 2017).

SPR was used for determining the parameters for PvRON2-RI and PvRON2-RII (immobilised ligands) binding to PvAMA1, PvAMA-DI-II, PvAMA-DII-III, PvRON4, and PvRON5 (as analytes). Equilibrium binding constant (kD) was calculated from association rate constant (k_{on}) and dissociation rate constant (k_{off}); both PvRON2-RI and PvRON2-RII bound specifically to PvAMA1 Domains II and III (i.e., PvAMA-DII-III) with kD of 11.7 and 19.8 nM, respectively (Figure 4, Table 1), indicating that both PvRON2 regions could independently establish a specific interaction with PvAMA1, having greater affinity for PvAMA-DII-III than for the whole PvAMA1 ectodomain or PvAMA-DI-II (Table 1).

Previous structural work concerning *P. falciparum*, *P. vivax*, and *T. gondii* AMA1 relationship with RON2 has convincingly shown AMA1 Domain II loop and some Domain I residues participating in interaction with RON2 located in the carboxyl terminal extreme (RON2sp1; Tonkin et al., 2011; Vulliez-Le Normand et al., 2012; Vulliez-Le Normand et al.,

TABLE 1 Dissociation equilibrium constants (kD) obtained from interactions between PvRON2-RI and PvRON2-RII as ligands having different *Plasmodium vivax* analytes

Ligand: PvRON2-RI			
Analyte	K_{on} (1/Ms) ^a	K_{off} (1/s) ^b	kD (M) ^c
PvAMA-DII-III	5.07×10^5	5.96×10^{-3}	1.17×10^{-8}
PvAMA-DI-II	4.21×10^c	2.29×10^{-3}	5.44×10^{-7}
PvAMA1	5.31×10^4	6.09×10^{-3}	1.15×10^{-7}
PvRON4	1.30×10^3	4.62×10^{-3}	3.56×10^{-6}
PvRON5	577	1.91×10^{-3}	3.31×10^{-6}
PvAMA1 F128A	1.47×10^5	5.0×10^{-3}	3.4×10^{-8}
PvAMA1 Y179A	1.28×10^5	4.93×10^{-3}	3.86×10^{-8}
Ligand: PvRON2-RII			
Analyte	K_{on} (1/Ms)	K_{off} (1/s)	kD (M)
PvAMA-DII-III	3.49×10^5	6.69×10^{-3}	1.92×10^{-8}
PvAMA1	8.64×10^3	1.15×10^{-2}	1.74×10^{-6}
PvRON4	6.44×10^3	2.92×10^{-3}	4.54×10^{-7}
PvRON5	2.19×10^3	7.93×10^{-3}	3.62×10^{-6}
PvAMA1 F128A	3.18×10^5	2.49×10^{-3}	7.83×10^{-9}
PvAMA1 Y179A	7.68×10^5	6.33×10^{-3}	8.24×10^{-8}

The strongest interactions are shown in bold.

^aComplex formation rate is represented by association constant (K_{on}).

^bComplex decay rate is represented by the dissociation constant (K_{off}).

^cInteraction dissociation constant (kD) was calculated from K_{on} and K_{off} .

2017). Such data have led to establishing that the Domain II loop causes an important conformational change, revealing a RON2 binding site, and becomes responsible for complex stability during invasion (Delgadillo, Parker, Lebrun, Boulanger, & Douguet, 2016). It should be stressed that even though PvRON2-RII (containing PvRON2sp1 binding to PvAMA1; Vulliez-Le Normand et al., 2017) bound specifically to PvAMA1 (1.74 μ M kD; Table 1) in the present work, such interaction had less affinity than that reported for the PvRON2sp1-PvAMA1 complex (50 nM kD; Vulliez-Le Normand et al., 2017). However, a stronger interaction was found for PvAMA-DII-III with PvRON2, suggesting other PvAMA1 regions' participation in the interaction with PvRON2. It should also be stressed that another PvRON2 functional region located towards the central region participates in interaction with reticulocytes (Figure 2) and also interacts strongly with PvAMA1 (Figure 4 and Table 1), as also proposed for *P. falciparum* (Hossain et al., 2012).

Guided by PfAMA1-PfRON2 structural studies, where some PfAMA1 (Phe183 and Tyr234) residues were seen to be key elements

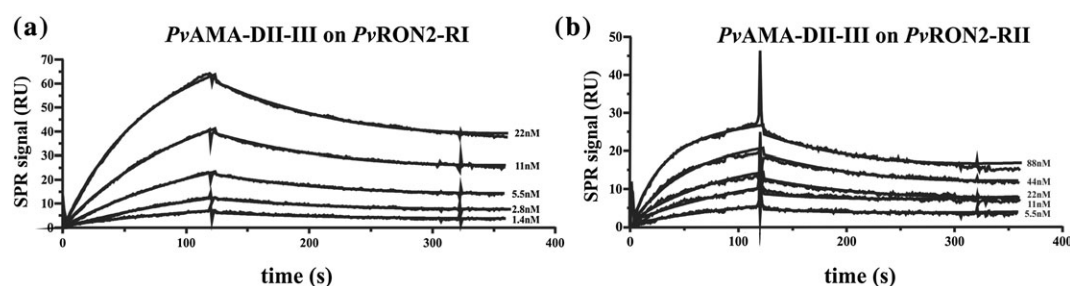


FIGURE 4 Measuring PvRON2-RI and PvRON2-RII interactions with PvAMA-DII-III by surface plasmon resonance. (a) Sensorgrams showing PvAMA-DII-III (analyte) binding to PvRON2-RI (immobilised). PvAMA-DII-III concentrations are indicated for each curve (nM). (b). Sensorgrams showing PvAMA-DII-III (analyte) binding to PvRON2-RII (immobilised), PvAMA-DII-III with concentrations indicated

in the interaction with *Pf*RON2sp1 (Vulliez-Le Normand et al., 2012), the *Pv*AMA1 Phe128 or Tyr179 homologous residues' functional importance was evaluated regarding interaction with *Pv*RON2-RI and *Pv*RON2-RII. Two soluble recombinant proteins were generated and purified by affinity chromatography (Supporting Information). Both mutant recombinant proteins were then used as analytes against *Pv*RON2-RI or *Pv*RON2-RII immobilised on sensor chip. Interestingly, both *Pv*AMA1 mutants displayed an order of magnitude increase in binding by SPR (10^{-7} vs. 10^{-8} kD; Table 1), which suggested that such residues are not essential for the interaction with *Pv*RON2, as opposed to what has been reported for their *P. falciparum* counterparts (*Pf*AMA1-*Pf*RON2; Vulliez-Le Normand et al., 2012).

It was found that both *Pv*RON2 regions interacted with *Pv*RON4 and *Pv*RON5 but with lower affinity than that reported for interaction with *Pv*AMA-DII-III. Previous *T. gondii* studies have shown that *Tg*RON5 stabilised *Tg*RON2 and that a loss of *Tg*RON4 significantly reduced *Tg*RON5 and *Tg*RON2 levels. Although it is not clear during which process such interaction might occur, the three proteins were located in the same compartment and released together during invasion. This does not rule out a transitory interaction during their stay in the rhoptry necks and subsequent organisation in host cell cytosol.

Altogether, these results highlight *Pv*RON2 and *Pv*RON4 importance in active *P. vivax* receptor-ligand and protein-protein complex formation as they could be key elements during parasite invasion. It was clear that *P. vivax* functional regions could be different to those involved in *P. falciparum*, despite these proteins' conservation in most Apicomplexa; this highlights important implications for designing an effective synthetic vaccine against *P. vivax*.

3 | EXPERIMENTAL PROCEDURES

3.1 | Recombinant plasmids

A gene fragment encoding a *Pv*RON4 region (residues 403–680) and two fragments encoding *Pv*RON2 (residues 957–1288 encoding RI and residues 1850–2085 RII) were amplified from *P. vivax* VCG-I strain complementary DNA (cDNA) for *Pv*RON4 and *Pv*RON2 expression as recombinant proteins in *E. coli* or expression on COS-7 cell membrane (American Type Culture Collection CRL-1651). Gene specific primers were designed using *pvrn4* (PVX_091434) and *pvrn2* cDNA sequences (PVX_117880) available in PlasmoDB as template (Urquiza et al., 2002). A KAPA HiFi HotStart ReadyMix PCR kit was used for amplifying each fragment at 25 µl final reaction volume, containing 12.5 µl 2× KAPA HiFi Ready Mix, 1.5 µl of each primer (Table S1) at 5 µM and 7.5 µl of nuclease-free water. The amplification conditions for the three products consisted of one 5-min cycle at 95 °C, followed by 35 cycles lasting 20 s at 98 °C, 45 s at 56 °C for *Pv*RON2 fragments or 60 °C for *Pv*RON4 fragments, and 2 min at 72 °C with a final extension cycle lasting 5 min at 72 °C.

Purified products were digested with *Pvu*II and *Ap*I restriction enzymes and cloned in pRE4 vector (Cohen et al., 1988) in frame with the HSVgD signal sequence and transmembrane segment (Chitnis & Miller, 1994) to express these fragments on COS-7 cell membrane or digested with *Bam*HI and *Sal*I for *Pv*RON4 or *Bam*HI and *Pst*I for the

*Pv*RON2-RII fragment. They were then cloned in pQE30 in frame with a histidine tag at the N-terminal to be expressed in *E. coli*, whereas the *Pv*RON2-RI amplified product was cloned in pEXP5-CT/TOPO expression vector using TOPO TA cloning in frame with a histidine tag at the C-terminus. Each construct was transformed in JM109 cells and selected on Luria Bertani (LB) plates containing ampicillin and confirmed by sequencing. Only the *Pv*RON2-RI plasmid was used to transform BL21DE3 cells and selected on LB plus ampicillin. The resulting plasmids were labelled pRE4-*Pv*RON4, pRE4-*Pv*RON2RI, pRE4-*Pv*RON2RII, pQE30-*Pv*RON4, pQE30-*Pv*RON2RII, and pEXP5-*Pv*RON2RI.

Recombinant plasmids encoding *Pv*AMA1 ectodomain, Domains I and II (*Pv*AMA1-DI-II), Domains II and III (*Pv*AMA-DII-III), and the C-terminal fragment of *Pv*RON5 were taken from previous studies to express such fragments in *E. coli* (Arevalo-Pinzon et al., 2015; Arevalo-Pinzon et al., 2017). The pHVDR22 plasmid was used to express the Duffy-binding Region II on COS-7 cell membrane as positive control (*Pv*DBP-RII; Chitnis & Miller, 1994).

3.2 | Transfecting COS-7 cells and immunofluorescence assays

COS-7 cells were cultured in Dulbecco-Modified Eagle Medium with 10% FCS in a humidified 5% CO₂ incubator at 37 °C. All transfection experiments involved using 3×10^4 cells seeded in 3.5-cm diameter wells (40–60% confluent) and then transfected with 300 ng of each recombinant plasmid using FuGENE HD transfection reagent (Promega), following the manufacturer's protocol. Transfected cells grown on coverslips were washed with phosphate buffered saline (PBS), and the immunofluorescence assay was done as described in previous studies (Arevalo-Pinzon et al., 2017; Chitnis & Miller, 1994). Fluorescence was visualised by fluorescence microscope (Olympus BX51) using an Olympus DP2 camera and Fiji software. Transfection efficiency (%) was calculated as total amount of fluorescent COS-7 cells \times 100/total amount of COS-7 cells counted in 30 fields, as described previously (Gao et al., 2008).

3.3 | Rosetting assays

Human UCB RBC, containing about 5–7% reticulocytes (*Fya*⁺*Fyb*[−]), were washed three times in PBS (pH 7.4) and then treated with neuraminidase, chymotrypsin, or trypsin, as described earlier (Curtidor et al., 2014). Briefly, an erythrocyte suspension (60% haematocrit) was incubated at 37 °C for 60 min with either neuraminidase (150 µU/mL; ICN 900-67-6), trypsin (1 mg/mL; Sigma T-1005), or chymotrypsin (1 mg/mL; Sigma C-4129). Erythrocytes were then washed twice by spinning with PBS at 2,500×g for 5 min. Untreated RBC having *Fya*⁺*Fyb*⁺, *Fya*[−]*Fyb*⁺, *Fya*⁺*Fyb*[−], *Fya*[−]*Fyb*[−] Duffy phenotypes were used for binding assays. The UCB used in this study came from Bogotá's Instituto Distrital de Ciencia, Biotecnología e Innovación en Salud (IDCBIS).

COS-7 cells, 48 hr after transfection with pRE4-*Pv*RON4 or pHVDR22 plasmids, were tested for binding to normal, neuraminidase-treated, chymotrypsin-treated, and trypsin-treated human UCB RBC (10%) or reticulocyte-depleted erythrocytes (10% haematocrit)

from peripheral blood without any treatment for 2 hr at 37 °C. Competition assays involved UCB (10%) preincubated with 10- μ l peptide 40305 (1 mg/ml) for 1 hr at 37 °C followed by two washes with incomplete Dulbecco-Modified Eagle Medium and then added to transfected COS-7 cells, as previously described (Arevalo-Pinzon et al., 2017). COS-7 cells with adherent erythrocytes or normocytes (i.e., rosettes) were scored in 20 randomly chosen fields at 200 \times magnification. Rosettes were considered positive when adherent erythrocytes covered more than 50% of COS-7 cell surface. COS-7 cells expressing PvDBP-RII on membrane were used as positive control (Chitnis & Miller, 1994) whilst the same cells but incubated with chymotrypsin-treated RBC or nontransfected cells were used as negative control. At least three independent experiments were performed with replicates.

3.4 | Obtaining and purifying recombinant proteins

E. coli (JM109) transformed with pQE30-PvAMA-1, pQE30-PvAMA-DI-II, pQE30-PvAMA-DII-III, pQE30-PvRON4, or pQE30-PvRON2RII, and *E. coli* BL21DE3 strain transformed with pEXP5-PvRON2RI or M15 cells transformed with pQE30-rRON5 were grown in 25-ml LB broth supplemented with 0.1-mg/ml ampicillin (JM109-BL21DE3-M15 cells), 25- μ g/ml kanamycin (M15 cells), and 0.1% D-glucose for 12 hr at 37 °C with constant shaking. This starting culture was used to inoculate 475-ml LB broth containing 0.1-mg/ml ampicillin, 25- μ g/ml kanamycin, and 0.1% D-glucose maintained at 37 °C with constant shaking until reaching 0.6–0.8 optical density (OD) at 620 nm. Recombinant protein expression was induced with isopropyl β -D1-thiogalactopyranoside (IPTG) at 1-mM final concentration.

Recombinant proteins rPvAMA-1, rPvAMA-DI-II, and rPvAMA-DII-III were obtained in soluble form, following previously described conditions (Arevalo-Pinzon et al., 2017); rPvRON4, rPvRON5, rPvRON2-RI, and rPvRON2-RII were expressed and purified according to a previous study (Arevalo-Pinzon et al., 2015), with some modifications. Briefly, 4–5 hr after IPTG induction, cell cultures were spun at 10,000 \times g for 30 min at 4 °C, and the bacterial pellet containing the protein in inclusion bodies was washed twice with buffer A (20-mM Tris-HCl pH 8.0, 1-mM EDTA, 1-mM iodoacetamide, 1-mM PMSF, and 1- μ g/ml leupeptin) supplemented with lysozyme, followed by cell disruption using a sonicator (Branson); 20-mM EDTA, 2% Triton X100, and 0.5-M NaCl were then added. Inclusion bodies were recovered by spinning at 10,000 \times g for 30 min at 4 °C and washed once with Buffer A. The recombinant protein was then solubilised with lysis buffer containing 10-mM Tris-HCl, 100-mM NaH₂PO₄, 4-M urea, 10-mM imidazole, and 10% glycerol. Western blot, using an antipolyhistidine monoclonal antibody (Sigma), was used for recognising recombinant proteins in supernatant.

The supernatant was incubated with nickel-nitrilotriacetic acid (Ni²⁺-NTA) agarose resin for purifying recombinant proteins by affinity chromatography. Bound protein was eluted with increasing imidazole gradients (50–500 mM). The eluates were analysed on SDS-PAGE and by western blot and the fractions containing the recombinant protein having a clear single band were pooled. Soluble proteins and those obtained with urea were exhaustively dialysed against 1X PBS. Protein concentration was determined using the BioRad protein assay system

(Bicinchoninic Acid Kit) and a standard bovine serum albumin curve. The presence of free thiol groups, if any, in the recombinant proteins was detected by using Ellman's reagent (5,5'-dithio-bis-3-nitrobenzoic acid; Thermo Scientific).

3.5 | PvRON2- and PvRON4-derived peptide synthesis and purification

Twenty-residue-long, nonoverlapping peptides derived from PvRON4 (15 peptides) and PvRON2 (17 peptides) sequences (Supporting Information) were chemically synthesised using solid-phase, multiple peptide synthesis, 4-methylbenzhydrylamine hydrochloride resin (0.5 meq/g), and t-Boc protected amino acids (Bachem; Houghten, 1985; Merrifield, 1963). The synthetic peptides were cleaved using low-high hydrogen fluoride cleavage. Peptides having greater than 99% purity were obtained by combining analytical reversed-phase high-performance liquid chromatography (RP-HPLC), semipreparative RP-HPLC, and matrix-assisted laser desorption/ionisation time-of-flight mass spectrometry (MALDI-ToF MS; Bruker Daltonics).

3.6 | Radiolabelling recombinant proteins and synthetic peptides

Briefly, 15- μ g PvRON2-RI or PvRON2-RII recombinant proteins were radiolabelled with 4- μ l of Na¹²⁵I (100 mCi/ml; ARC) and Iodination Beads (Pierce-Thermo Scientific), following the manufacturer's instructions. Following 12-min incubation, radiolabelled recombinant proteins were separated by solution throughout on a SigmaSpin column; 3- μ l - Na¹²⁵I (100 mCi/ml; ARC) and 25- μ l chloramine T (2.75 mg/ml) were used for radiolabelling the synthetic peptides. The reaction was stopped after 15 min by adding 25- μ l sodium metabisulphite (2.3 mg/ml), as described previously (Arevalo-Pinzon et al., 2013). Radiolabelled peptides were separated by size-exclusion chromatography on a Sephadex G-25 column (Pharmacia). Each eluted fraction was then analysed by gamma counter (Packard Cobra II).

3.7 | Radiolabelling proteins and peptide binding assays

Briefly, 2×10^7 UCB RBC were incubated at room temperature (RT) for 90 min with different concentrations of each radiolabelled recombinant protein (0–400 nM) or radiolabelled peptide (0–800 nM) in the absence (total binding) or presence (non-specific binding) of the same unlabelled recombinant protein or unlabelled peptide (200 μ l final volume). Competition assays involved adding each PvRON4- and PvRON2-RI-derived synthetic peptide (Supporting Information), at a 1:100 (labelled protein:unlabelled peptide) molar ratio. Following incubation, cells were washed twice with HBS, and the amount of cell-bound radiolabelled recombinant protein or peptide was quantified on an automatic gamma counter.

Peptides' specific binding activity was evaluated in a binding assay with enzyme-treated UCB RBC; 2×10^7 untreated RBC and trypsin-, chymotrypsin-, or neuraminidase-treated RBC were incubated at RT for 90 min with 400 nM of each radiolabelled peptide in the absence

or presence of the same unlabelled peptide, as described previously (Arevalo-Pinzon, Curtidor, Munoz, et al., 2013).

3.8 | Flow cytometry binding assays

Flow cytometry assays were carried out according to previously described protocols (Arevalo-Pinzon et al., 2017; Moreno-Perez, Baquero, Chitiva-Ardila, & Patarroyo, 2017). Briefly, 25- μ g PvRON4 or PvRON2-RI recombinant protein were incubated with 5% UCB RBC and then incubated with antibodies against the transferrin receptor (CD71) on reticulocytes, against cluster of differentiation 45 (CD45) in leukocytes (some activated leukocytes are CD71⁺, but reticulocytes are CD45⁻, so the reticulocyte population selected was CD71⁺ CD45⁻) and antibodies against the 6X-His-tag in recombinant proteins. UCB RBC were preincubated with peptides before adding recombinant protein for competition assays with peptides 40305 and 40595. The events were acquired on a FACSCanto II (BD Bioscience); results were analysed using FlowJo software (TreeStar). DBP-RII recombinant soluble protein was used as positive binding control and DBP-RIII-IV as negative control. At least three independent experiments were performed with different UCB samples.

3.9 | Surface plasmon resonance

SPR involved using BIACORE 3000 system (Uppsala, Sweden), sensor chip CM5 (GE Healthcare Life Sciences), surfactant P20, and amine coupling kit containing N-hydroxysuccinimide (NHS) and N-Ethyl-N'-dimethylaminopropyl carbodiimide (EDC). All biosensor assays were performed with HEPES-buffered saline (HBS-P) as running buffer (10-mM HEPES, 150-mM sodium acetate, 3-mM magnesium acetate, 0.005% surfactant P20, and 5-mM CaCl₂, pH 7.4). Compounds were dissolved in running buffer. Immobilisations were performed by injecting 40- μ l PvRON2-RI and PvRON2-RII (100 μ g/ml in formate buffer, pH 4.3) onto a CM5 sensor chip's activated surface by EDC/NHS, giving 300 RU (PvRON2-RI) and 1,500 (PvRON2-RII) RU signal, followed by 20- μ l ethanolamine hydrochloride, pH 8.5, to saturate the matrix's free activated sites.

Increasing concentrations of each purified analyte (PvAMA1, PvAMA-DI-II, PvAMA-DII-III, PvRON4, PvAMA1^{F128A}, PvAMA1^{Y179A}, and PvRON5) were injected at constant 30 μ l/min flow rate at 25 °C. The sensor chip surface was regenerated after each experiment by injecting 20 μ l 10 mM HCl. BIAeval 4.1 software was used for calculating kinetic parameters. A simple Langmuir binding model was used for overall analysis. The specific binding profiles were obtained after subtracting the response signal from the channel control (activated/deactivated by ethanolamine). Fitting to each model was judged by reduced chi square test values and residue distribution randomness.

3.10 | Statistical analysis

SPSS v20.0 was used for statistical analysis of RBC-binding assays. Mean values and standard deviations (SD) were calculated from the measurements of three independent experiments. Student's *t* test and analysis of variance (ANOVA) were used for comparing the means of each experimental group using a 0.05 significance level for testing a

stated hypothesis. Tukey's multiple comparison test was used for multiple comparison of experimental group means to those for control.

3.11 | Ethical approval and consent to participate

All the parents of the donors of the UCB samples used here signed an informed consent form after receiving detailed information regarding the study's goals. The UCB samples were collected by Bogotá's Instituto Distrital de Ciencia, Biotecnología e Innovación en Salud (IDCBIS), following the protocols established by this institution, and in accordance with Colombian laws and regulations. All procedures were approved by FIDIC's ethics committee.

ACKNOWLEDGEMENTS

We are grateful to Prof. Asif Mohammed and Prof. Chetan E. Chitnis from the International Centre for Genetic Engineering and Biotechnology (New Delhi, India) for providing pRE4 and pHVDR22 plasmids. We would like to thank Dr. Bernardo Camacho and Dr. Ana María Perdomo from the Instituto Distrital de Ciencia, Biotecnología e Innovación en Salud (IDCBIS), for providing UCB and also Jason Garry for translating this manuscript. This research was financed by the Colombian Science, Technology, and Innovation Department (COLCIENCIAS) through the contract RC#0309-2013 and in part, by the French Centre National de la Recherche Scientifique (CNRS), the Laboratory of Excellence Medalis (ANR-10-LABX-0034), Initiative of Excellence (IdEx), Strasbourg University, France. GAP was financed by COLCIENCIAS' National Call for PhD Studies in Colombia (No. 567). M. B. was financed by the "High level human talent training" project, approved by the Colombian General Royalties System's (GRS) "Science, Technology and Innovation Fund" (CTel) BPIN 2013000100103, Tolima Department's Governor's Office and by the Universidad del Tolima, Colombia. The sponsors had no role in study design or data collection, analysis, and/or interpretation.

CONFLICT OF INTEREST STATEMENT

The authors declare that the research was conducted in the absence of any commercial or financial relationships that could be construed as a potential conflict of interest.

ORCID

Manuel Alfonso Patarroyo  <http://orcid.org/0000-0002-4751-2500>

REFERENCES

- Aikawa, M., Miller, L. H., Johnson, J., & Rabbage, J. (1978). Erythrocyte entry by malarial parasites. A moving junction between erythrocyte and parasite. *The Journal of Cell Biology*, 77, 72–82.
- Alexander, D. L., Arastu-Kapur, S., Dubremetz, J. F., & Boothroyd, J. C. (2006). Plasmodium falciparum AMA1 binds a rhoptry neck protein homologous to TgRON4, a component of the moving junction in Toxoplasma gondii. *Eukaryotic Cell*, 5, 1169–1173.
- Alexander, D. L., Mital, J., Ward, G. E., Bradley, P., & Boothroyd, J. C. (2005). Identification of the moving junction complex of Toxoplasma gondii: A collaboration between distinct secretory organelles. *PLoS Pathogens*, 1, e17.
- Arevalo-Pinzon, G., Bermudez, M., Curtidor, H., & Patarroyo, M. A. (2015). The Plasmodium vivax rhoptry neck protein 5 is expressed in the apical

- pole of *Plasmodium vivax* VCG-1 strain schizonts and binds to human reticulocytes. *Malaria Journal*, 14, 106.
- Arevalo-Pinzon, G., Bermudez, M., Hernandez, D., Curtidor, H., & Patarroyo, M. A. (2017). *Plasmodium vivax* ligand-receptor interaction: PvAMA-1 domain I contains the minimal regions for specific interaction with CD71+ reticulocytes. *Scientific Reports*, 7, 9616.
- Arevalo-Pinzon, G., Curtidor, H., Abril, J., & Patarroyo, M. A. (2013). Annotation and characterization of the *Plasmodium vivax* rhoptry neck protein 4 (PvRON4). *Malaria Journal*, 12, 356.
- Arevalo-Pinzon, G., Curtidor, H., Munoz, M., Suarez, D., Patarroyo, M. A., & Patarroyo, M. E. (2013). Rh1 high activity binding peptides inhibit high percentages of *Plasmodium falciparum* FVO strain invasion. *Vaccine*, 31, 1830–1837.
- Arevalo-Pinzon, G., Curtidor, H., Patino, L. C., & Patarroyo, M. A. (2011). PvRON2, a new *Plasmodium vivax* rhoptry neck antigen. *Malaria Journal*, 10, 60.
- Baquero, L. A., Moreno-Perez, D. A., Garzon-Ospina, D., Forero-Rodriguez, J., Ortiz-Suarez, H. D., & Patarroyo, M. A. (2017). PvGAMA reticulocyte binding activity: Predicting conserved functional regions by natural selection analysis. *Parasites & Vectors*, 10, 251.
- Bargieri, D. Y., Andenmatten, N., Lagal, V., Thiberge, S., Whitelaw, J. A., Tardieux, I., ... Ménard, R. (2013). Apical membrane antigen 1 mediates apicomplexan parasite attachment but is dispensable for host cell invasion. *Nature Communications*, 4, 2552.
- Barnwell, J. W., Nichols, M. E., & Rubinstein, P. (1989). In vitro evaluation of the role of the Duffy blood group in erythrocyte invasion by *Plasmodium vivax*. *The Journal of Experimental Medicine*, 169, 1795–1802.
- Beck, J. R., Chen, A. L., Kim, E. W., & Bradley, P. J. (2014). RON5 is critical for organization and function of the *Toxoplasma* moving junction complex. *PLoS Pathogens*, 10, e1004025.
- Berntzen, G., Lunde, E., Flobakk, M., Andersen, J. T., Lauvraak, V., & Sandlie, I. (2005). Prolonged and increased expression of soluble Fc receptors, IgG and a TCR-Ig fusion protein by transiently transfected adherent 293E cells. *Journal of Immunological Methods*, 298, 93–104.
- Besteiro, S., Michelin, A., Poncet, J., Dubremetz, J. F., & Lebrun, M. (2009). Export of a *Toxoplasma gondii* rhoptry neck protein complex at the host cell membrane to form the moving junction during invasion. *PLoS Pathogens*, 5, e1000309.
- Bozdech, Z., Mok, S., Hu, G., Imwong, M., Jaidee, A., Russell, B., ... Preiser, P. R. (2008). The transcriptome of *Plasmodium vivax* reveals divergence and diversity of transcriptional regulation in malaria parasites. *Proceedings of the National Academy of Sciences of the United States of America*, 105, 16290–16295.
- Bradley, P. J., Ward, C., Cheng, S. J., Alexander, D. L., Collier, S., Coombs, G. H., ... Boothroyd, J. C. (2005). Proteomic analysis of rhoptry organelles reveals many novel constituents for host-parasite interactions in *Toxoplasma gondii*. *The Journal of Biological Chemistry*, 280, 34245–34258.
- Buitrago, S. P., Garzon-Ospina, D., & Patarroyo, M. A. (2016). Size polymorphism and low sequence diversity in the locus encoding the *Plasmodium vivax* rhoptry neck protein 4 (PvRON4) in Colombian isolates. *Malaria Journal*, 15, 501.
- Cao, J., Kaneko, O., Thongkukiatkul, A., Tachibana, M., Otsuki, H., Gao, Q., ... Torii, M. (2009). Rhoptry neck protein RON2 forms a complex with microneme protein AMA1 in *Plasmodium falciparum* merozoites. *Parasitology International*, 58, 29–35.
- Carruthers, V. B. (2002). Host cell invasion by the opportunistic pathogen *Toxoplasma gondii*. *Acta Tropica*, 81, 111–122.
- Chitnis, C. E., & Miller, L. H. (1994). Identification of the erythrocyte binding domains of *Plasmodium vivax* and *Plasmodium knowlesi* proteins involved in erythrocyte invasion. *The Journal of Experimental Medicine*, 180, 497–506.
- Cohen, G. H., Wilcox, W. C., Sodora, D. L., Long, D., Levin, J. Z., & Eisenberg, R. J. (1988). Expression of herpes simplex virus type 1 glycoprotein D deletion mutants in mammalian cells. *Journal of Virology*, 62, 1932–1940.
- Collins, C. R., Withers-Martinez, C., Hackett, F., & Blackman, M. J. (2009). An inhibitory antibody blocks interactions between components of the malarial invasion machinery. *PLoS Pathogens*, 5, e1000273.
- Counihan, N. A., Kalanon, M., Coppel, R. L., & de Koning-Ward, T. F. (2013). *Plasmodium* rhoptry proteins: Why order is important. *Trends in Parasitology*, 29, 228–236.
- Curtidor, H., Patarroyo, M. E., & Patarroyo, M. A. (2015). Recent advances in the development of a chemically synthesised anti-malarial vaccine. *Expert Opinion on Biological Therapy*, 15, 1567–1581.
- Curtidor, H., Patino, L. C., Arevalo-Pinzon, G., Patarroyo, M. E., & Patarroyo, M. A. (2011). Identification of the *Plasmodium falciparum* rhoptry neck protein 5 (PvRON5). *Gene*, 474, 22–28.
- Curtidor, H., Patino, L. C., Arevalo-Pinzon, G., Vanegas, M., Patarroyo, M. E., & Patarroyo, M. A. (2014). *Plasmodium falciparum* rhoptry neck protein 5 peptides bind to human red blood cells and inhibit parasite invasion. *Peptides*, 53, 210–217.
- Curtidor, H., Vanegas, M., Alba, M. P., & Patarroyo, M. E. (2011). Functional, immunological and three-dimensional analysis of chemically synthesised sporozoite peptides as components of a fully-effective antimalarial vaccine. *Current Medicinal Chemistry*, 18, 4470–4502.
- Deans, J. A., Alderson, T., Thomas, A. W., Mitchell, G. H., Lennox, E. S., & Cohen, S. (1982). Rat monoclonal antibodies which inhibit the in vitro multiplication of *Plasmodium knowlesi*. *Clinical and Experimental Immunology*, 49, 297–309.
- Delgadillo, R. F., Parker, M. L., Lebrun, M., Boulanger, M. J., & Douguet, D. (2016). Stability of the *Plasmodium falciparum* AMA1-RON2 complex is governed by the domain II (DII) loop. *PLoS One*, 11, e0144764.
- DeSimone, T. M., Jennings, C. V., Bei, A. K., Comeaux, C., Coleman, B. I., Refour, P., ... Duraisingh, M. T. (2009). Cooperativity between *Plasmodium falciparum* adhesive proteins for invasion into erythrocytes. *Molecular Microbiology*, 72, 578–589.
- Diaz, S. A., Martin, S. R., Howell, S. A., Grainger, M., Moon, R. W., Green, J. L., & Holder, A. A. (2016). The binding of *Plasmodium falciparum* Adhesins and erythrocyte invasion proteins to aldolase is enhanced by phosphorylation. *PLoS One*, 11, e0161850.
- Duraisingh, M. T., Maier, A. G., Triglia, T., & Cowman, A. F. (2003). Erythrocyte-binding antigen 175 mediates invasion in *Plasmodium falciparum* utilizing sialic acid-dependent and -independent pathways. *Proceedings of the National Academy of Sciences of the United States of America*, 100, 4796–4801.
- Duraisingh, M. T., Triglia, T., Ralph, S. A., Rayner, J. C., Barnwell, J. W., McFadden, G. I., & Cowman, A. F. (2003). Phenotypic variation of *Plasmodium falciparum* merozoite proteins directs receptor targeting for invasion of human erythrocytes. *The EMBO Journal*, 22, 1047–1057.
- Gao, X., Yeo, K. P., Aw, S. S., Kuss, C., Iyer, J. K., Genesan, S., ... Preiser, P. R. (2008). Antibodies targeting the PFRH1 binding domain inhibit invasion of *Plasmodium falciparum* merozoites. *PLoS Pathogens*, 4, e1000104.
- Gilberger, T. W., Thompson, J. K., Triglia, T., Good, R. T., Duraisingh, M. T., & Cowman, A. F. (2003). A novel erythrocyte binding antigen-175 paralogue from *Plasmodium falciparum* defines a new trypsin-resistant receptor on human erythrocytes. *The Journal of Biological Chemistry*, 278, 14480–14486.
- Giovannini, D., Spath, S., Lacroix, C., Perazzi, A., Bargieri, D., Lagal, V., ... Ménard, R. (2011). Independent roles of apical membrane antigen 1 and rhoptry neck proteins during host cell invasion by apicomplexa. *Cell Host & Microbe*, 10, 591–602.
- Gruszczyk, J., Kanjee, U., Chan, L. J., Menant, S., Malleret, B., Lim, N. T. Y., ... Tham, W. H. (2018). Transferrin receptor 1 is a reticulocyte-specific receptor for *Plasmodium vivax*. *Science*, 359, 48–55.
- Guerin, A., Corrales, R. M., Parker, M. L., Lamarque, M. H., Jacot, D., El Hajj, H., ... Lebrun, M. (2017). Efficient invasion by *Toxoplasma* depends on the subversion of host protein networks. *Nature Microbiology*, 2, 1358–1366.
- Hossain, M. E., Dhawan, S., & Mohammed, A. (2012). The cysteine-rich regions of *Plasmodium falciparum* RON2 bind with host erythrocyte

- and AMA1 during merozoite invasion. *Parasitology Research*, 110, 1711–1721.
- Houghten, R. A. (1985). General method for the rapid solid-phase synthesis of large numbers of peptides: Specificity of antigen-antibody interaction at the level of individual amino acids. *Proceedings of the National Academy of Sciences of the United States of America*, 82, 5131–5135.
- Howes, R. E., Battle, K. E., Mendis, K. N., Smith, D. L., Cibulskis, R. E., Baird, J. K., & Hay, S. I. (2016). Global epidemiology of *Plasmodium vivax*. *The American Journal of Tropical Medicine and Hygiene*, 95, 15–34.
- Kato, K., Mayer, D. C., Singh, S., Reid, M., & Miller, L. H. (2005). Domain III of *Plasmodium falciparum* apical membrane antigen 1 binds to the erythrocyte membrane protein Kx. *Proceedings of the National Academy of Sciences of the United States of America*, 102, 5552–5557.
- Lamarque, M., Besteiro, S., Papoin, J., Roques, M., Vulliez-Le Normand, B., Morlon-Guyot, J., ... Lebrun, M. (2016). The RON2-AMA1 interaction is a critical step in moving junction-dependent invasion by apicomplexan parasites. *PLoS Pathogens*, 7, e1001276.
- Lamarque, M. H., Roques, M., Kong-Hap, M., Tonkin, M. L., Rugarabamu, G., Marq, J. B., ... Lebrun, M. (2014). Plasticity and redundancy among AMA-RON pairs ensure host cell entry of *Toxoplasma* parasites. *Nature Communications*, 5, 4098.
- Lopatnicki, S., Maier, A. G., Thompson, J., Wilson, D. W., Tham, W. H., Triglia, T., ... Cowman, A. F. (2011). Reticulocyte and erythrocyte binding-like proteins function cooperatively in invasion of human erythrocytes by malaria parasites. *Infection and Immunity*, 79, 1107–1117.
- Merrifield, R. B. (1963). Solid phase peptide synthesis. I. The synthesis of a tetrapeptide. *Journal of the American Chemical Society*, 85, 2149–2154.
- Miller, L. H., Mason, S. J., Clyde, D. F., & McGinniss, M. H. (1976). The resistance factor to *Plasmodium vivax* in blacks. The Duffy-blood-group genotype, FyFy. *The New England Journal of Medicine*, 295, 302–304.
- Mital, J., Meissner, M., Soldati, D., & Ward, G. E. (2005). Conditional expression of *Toxoplasma gondii* apical membrane antigen-1 (TgAMA1) demonstrates that TgAMA1 plays a critical role in host cell invasion. *Molecular Biology of the Cell*, 16, 4341–4349.
- Mitchell, G. H., Thomas, A. W., Margos, G., Dlugowski, A. R., & Bannister, L. H. (2004). Apical membrane antigen 1, a major malaria vaccine candidate, mediates the close attachment of invasive merozoites to host red blood cells. *Infection and Immunity*, 72, 154–158.
- Moreno-Perez, D. A., Baquero, L. A., Chitiva-Ardila, D. M., & Patarroyo, M. A. (2017). Characterising PvRBSA: An exclusive protein from *Plasmodium* species infecting reticulocytes. *Parasites & Vectors*, 10, 243.
- Moreno-Perez, D. A., Degano, R., Ibarrola, N., Muro, A., & Patarroyo, M. A. (2014). Determining the *Plasmodium vivax* VCG-1 strain blood stage proteome. *Journal of Proteomics*, 113C, 268–280.
- Ntumngia, F. B., Thomson-Luque, R., Torres Lde, M., Gunalan, K., Carvalho, L. H., & Adams, J. H. (2016). A novel erythrocyte binding protein of *Plasmodium vivax* suggests an alternate invasion pathway into Duffy-positive reticulocytes. *MBio*, 7, e01261–e01216.
- Ocampo, M., Vera, R., Eduardo Rodriguez, L., Curtidor, H., Urquiza, M., Suarez, J., ... Elkin Patarroyo, M. (2002). *Plasmodium vivax* Duffy binding protein peptides specifically bind to reticulocytes. *Peptides*, 23, 13–22.
- Ovchinnikova, E., Aglialoro, F., Bentlage, A. E. H., Vidarsson, G., Salinas, N. D., von Lindern, M., ... van den Akker, E. (2017). DARC extracellular domain remodeling in maturing reticulocytes explains *Plasmodium vivax* tropism. *Blood*, 130, 1441–1444.
- Patarroyo, M. E., Bermudez, A., Alba, M. P., Vanegas, M., Moreno-Vranich, A., Poloch, L. A., & Patarroyo, M. A. (2015). IMPIPS: The immune protection-inducing protein structure concept in the search for steric-electron and topochemical principles for complete fully-protective chemically synthesised vaccine development. *PLoS One*, 10, e0123249.
- Patarroyo, M. A., Calderon, D., & Moreno-Perez, D. A. (2012). Vaccines against *Plasmodium vivax*: A research challenge. *Expert Review of Vaccines*, 11, 1249–1260.
- Pico de Coana, Y., Rodriguez, J., Guerrero, E., Barrero, C., Rodriguez, R., Mendoza, M., & Patarroyo, M. A. (2003). A highly infective *Plasmodium vivax* strain adapted to Aotus monkeys: Quantitative haematological and molecular determinations useful for *P. vivax* malaria vaccine development. *Vaccine*, 21, 3930–3937.
- Remarque, E. J., Faber, B. W., Kocken, C. H., & Thomas, A. W. (2008). Apical membrane antigen 1: a malaria vaccine candidate in review. *Trends in Parasitology*, 24, 74–84.
- Rodriguez, L. E., Curtidor, H., Urquiza, M., Cifuentes, G., Reyes, C., & Patarroyo, M. E. (2008). Intimate molecular interactions of *P. falciparum* merozoite proteins involved in invasion of red blood cells and their implications for vaccine design. *Chemical Reviews*, 108, 3656–3705.
- Rodriguez, L. E., Urquiza, M., Ocampo, M., Curtidor, H., Suarez, J., Garcia, J., ... Patarroyo, M. E. (2002). *Plasmodium vivax* MSP-1 peptides have high specific binding activity to human reticulocytes. *Vaccine*, 20, 1331–1339.
- Srinivasan, P., Beatty, W. L., Diouf, A., Herrera, R., Ambroggio, X., Moch, J. K., ... Miller, L. H. (2011). Binding of *Plasmodium* merozoite proteins RON2 and AMA1 triggers commitment to invasion. *Proceedings of the National Academy of Sciences of the United States of America*, 108, 13275–13280.
- Srinivasan, P., Ekanem, E., Diouf, A., Tonkin, M. L., Miura, K., Boulanger, M. J., ... Miller, L. H. (2014). Immunization with a functional protein complex required for erythrocyte invasion protects against lethal malaria. *Proceedings of the National Academy of Sciences of the United States of America*, 111, 10311–10316.
- Srinivasan, P., Yasgar, A., Luci, D. K., Beatty, W. L., Hu, X., Andersen, J., ... Miller, L. H. (2013). Disrupting malaria parasite AMA1-RON2 interaction with a small molecule prevents erythrocyte invasion. *Nature Communications*, 4, 2261.
- Straub, K. W., Cheng, S. J., Sohn, C. S., & Bradley, P. J. (2009). Novel components of the Apicomplexan moving junction reveal conserved and coccidia-restricted elements. *Cellular Microbiology*, 11, 590–603.
- Straub, K. W., Peng, E. D., Hajagos, B. E., Tyler, J. S., & Bradley, P. J. (2011). The moving junction protein RON8 facilitates firm attachment and host cell invasion in *Toxoplasma gondii*. *PLoS Pathogens*, 7, e1002007.
- Takemae, H., Sugi, T., Kobayashi, K., Gong, H., Ishiwa, A., Recuenco, F. C., ... Kato, K. (2013). Characterization of the interaction between *Toxoplasma gondii* rhoptry neck protein 4 and host cellular beta-tubulin. *Scientific Reports*, 3, 3199.
- Tonkin, M. L., Roques, M., Lamarque, M. H., Pugniere, M., Douguet, D., Crawford, J., ... Boulanger, M. J. (2011). Host cell invasion by apicomplexan parasites: Insights from the co-structure of AMA1 with a RON2 peptide. *Science*, 333, 463–467.
- Triglia, T., Healer, J., Caruana, S. R., Hodder, A. N., Anders, R. F., Crabb, B. S., & Cowman, A. F. (2000). Apical membrane antigen 1 plays a central role in erythrocyte invasion by *Plasmodium* species. *Molecular Microbiology*, 38, 706–718.
- Urquiza, M., Patarroyo, M. A., Mari, V., Ocampo, M., Suarez, J., Lopez, R., ... Patarroyo, M. E. (2002). Identification and polymorphism of *Plasmodium vivax* RBP-1 peptides which bind specifically to reticulocytes. *Peptides*, 23, 2265–2277.
- Urquiza, M., Suarez, J. E., Cardenas, C., Lopez, R., Puentes, A., Chavez, F., ... Patarroyo, M. E. (2000). *Plasmodium falciparum* AMA-1 erythrocyte binding peptides implicate AMA-1 as erythrocyte binding protein. *Vaccine*, 19, 508–513.
- Venkatesh, A., Patel, S. K., Ray, S., Shastri, J., Chatterjee, G., Kochar, S. K., ... Srivastava, S. (2016). Proteomics of *Plasmodium vivax* malaria: New insights, progress and potential. *Expert Review of Proteomics*, 13, 771–782.
- Vulliez-Le Normand, B., Saul, F. A., Hoos, S., Faber, B. W., & Bentley, G. A. (2017). Cross-reactivity between apical membrane antigen 1 and rhoptry neck protein 2 in *P. vivax* and *P. falciparum*: A structural and binding study. *PLoS One*, 12, e0183198.
- Vulliez-Le Normand, B., Tonkin, M. L., Lamarque, M. H., Langer, S., Hoos, S., Roques, M., ... Lebrun, M. (2012). Structural and functional insights into

- the malaria parasite moving junction complex. *PLoS Pathogens*, 8, e1002755.
- Weiss, G. E., Crabb, B. S., & Gilson, P. R. (2016). Overlaying molecular and temporal aspects of malaria parasite invasion. *Trends in Parasitology*, 32, 284–295.
- Weiss, G. E., Gilson, P. R., Taechalerpaisarn, T., Tham, W. H., de Jong, N. W., Harvey, K. L., ... Crabb, B. S. (2015). Revealing the sequence and resulting cellular morphology of receptor-ligand interactions during *Plasmodium falciparum* invasion of erythrocytes. *PLoS Pathogens*, 11, e1004670.
- Yap, A., Azevedo, M. F., Gilson, P. R., Weiss, G. E., O'Neill, M. T., Wilson, D. W., ... Cowman, A. F. (2014). Conditional expression of apical membrane antigen 1 in *Plasmodium falciparum* shows it is required for erythrocyte invasion by merozoites. *Cellular Microbiology*, 16, 642–656.

SUPPORTING INFORMATION

Additional Supporting Information may be found online in the supporting information tab for this article.

How to cite this article: Bermúdez M, Arévalo-Pinzón G, Rubio L, et al. Receptor–ligand and parasite protein–protein interactions in *Plasmodium vivax*: Analysing rhoptry neck proteins 2 and 4. *Cellular Microbiology*. 2018;20:e12835. <https://doi.org/10.1111/cmi.12835>